ISSN 0915-633X

NATIONAL INSTITUTE FOR FUSION SCIENCE

Global Simulation of the Magnetosphere with a Long Tail: The Formation and Ejection of Plasmoids

A. Kageyama, K. Watanabe and T. Sato

(Received – Sep. 6, 1990)

NIFS-49 Sep. 1990

RESEARCH REPORT
NIFS Series

NAGOYA, JAPAN

Global simulation of the magnetosphere with a long tail: The formation and ejection of plasmoids

A. Kageyama

Faculty of Science, Hiroshima University, Hiroshima 730, Japan

K. Watanabe and T. Sato

Theory and computer simulation center, National Institute for Fusion Science, Nagoya 464-01, Japan

Abstract

A global simulation of the formation of the magnetosphere with along tail is performed. A magnetosphere with a neutral sheet is constructed from a dipole field by solar wind dynamic pressure (no IMF). Subsequently, magnetic reconnection occurs in the plasma sheet and a large lump of plasma surrounded by reconnected field lines, a plasmoid, is formed and ejected tailward. The time scale of the plasmoid formation and ejection process is several hours. After ejecting the plasmoid, reconnection occurs again in the plasma sheet and the second plasmoid is formed and ejected. This result shows that the magnetosphere which has a sufficiently long tail and a neutral sheet is slightly unstable even though a solar wind does not contain an IMF.

Keywords; computer simulation, magnetohydrodynamics, magnetosphere, magnetotail, plasmoid, magnetic reconnection, plasma sheet

1 Introduction

The solar wind is a super Alfvénic flow. This means that the energy of the solar wind's magnetic field (the interplanetary magnetic field = IMF) is much lower than the energy of the solar wind plasma flow or dynamic energy. Thus, it is the solar wind's dynamic pressure that deforms the Earth's intrinsic dipole field into the shape of the magnetosphere. On the other hand, the IMF is believed to play an important role in magnetosphere dynamics, especially in magnetospheric substorms, through (dayside/nightside) magnetic reconnection processes.

Since the late 1950's, many spacecrafts have been launched to observe, directly, the magnetospheric plasma and field and have sent us abundant information. Even so, the magnetosphere is very large whereas data from single spacecraft observations are quite limited. One cannot infer the entire structure of the magnetosphere nor its global dynamics from these data.

Computer simulations appeared in the middle of the 1960's as a powerful means of studying magnetospheric physics. With computers, one can directly investigate a highly non-linear phenomena in the magnetosphere. For example, Hayashi and Sato [1978] performed a two dimensional simulation using the magnetohydrodynamic (MHD) equations and revealed that stored magnetic energy can be converted into plasma bulk flow energy and heat through magnetic reconnection within very short time scales. Accordingly, magnetic reconnection is thought to play an important role in magnetospheric substorms, which are rapid energy relaxation processes in the magnetosphere.

Hayashi and Sato's simulation is categorized as a local simulation. In a local simulation, one extracts a small region of the magnetosphere in which important processes occur in order to investigate the processes in detail. In reality, the chosen region exchanges energy and information through complex interactions with other regions of the magnetosphere. In a local simulation, these interactions are ignored or merely described by boundary conditions.

Recent advances in the speed and memory size of supercomputers enable us to directly simulate the whole magnetosphere, a global simulation. In a global simulation, one takes a large simulation box that involves the entire magnetosphere using a minimum of assumptions regarding the initial and boundary conditions.

Solar wind-magnetosphere coupling as well as processes within the magnetoshere are taken into account.

Watanabe and Sato [1990] performed a global simulation of the magnetosphere which extended the simulation region to $60Re$ in the tailward direction from the earth where $1Re$ is the length of the earth's radii. They used a high-precision three dimensional MHD code that revealed formation processes of the bow shock, magnetopause, plasma sheet and tail as well as showing the three dimensional structure of the magnetosphere. In their simulation the magnetosphere finally reaches a stationary state when the IMF is not considered. In that state, however, strong vertical magnetic field lines exist throughout the equatorial plane so that the magnetosphere in their simulation did not have a neutral sheet. It appears that a simulation region only up to $60Re$ in the tailward direction is not sufficiently large to simulate the magnetosphere.

In the current study, we have performed a global simulation of the magnetosphere, using the same high-precision 3-D MHD code as Watanabe and Sato and have extended the simulation box in the tailward direction to $100Re$ from the earth. Despite the above mentioned advances in computer memory size, we are still limited in grid number. Therefore, unlike Watanabe and Sato, who used an evenly spaced grid size throughout the simulation region, we adopted an unevenly spaced grid to extend the simulation region while maintaining numerical accuracy. This extension enabled us to obtain a more realistic magnetoshere with a sufficiently long tail and a neutral sheet.

Our main interest is determining whether or not this magnetosphere configuration is stable in the time scale of several hours when no IMF is present. In reality, the IMF is never continuously zero for more than one hour. So, this is an idealized problem. However, it provides an important basis for the study of the effects of the IMF on magnetosphere dynamics which will follow this work.

We will show that this magnetosphere is unstable though the growth rate of the instability is rather small. As soon as the magnetosphere formation is completed, the north lobe field and the south lobe field begin to reconnect in the plasma sheet at about $20Re$ behind the Earth (near-earth reconnection). As a result of this reconnection, a large lump of plasma surrounded by reconnected field lines, a plasmoid, is produced and ejected tailward. We show time sequences

of plasmoid ejections and the three dimensional structure of plasmoids.

The results we obtained are very similar to the processes predicted by the 'near-earth reconnection' or 'plasmoid' model of magnetospheric substorms. This model, originally proposed by Hones [1977], is supported by many observations [Slavin et al., 1989]. However, as mentioned above, the IMF is thought to play an important role in magnetospheric substorms. Observations indicate that magnetospheric substorms are often preceded by a southward turning of the IMF followed by an increase in the magnetic energy of the lobes. So, this is not a direct study of magnetospheric substorms but rather one of an idealized process which will provide a basis to the complete understanding of its mechanism.

2 Simulation Model

The macroscopic nature of magnetospheric plasmas is well described by the MHD equations.

$$\begin{aligned} \partial\rho/\partial t &= -\nabla\cdot(\rho\mathbf{v}) \\ \partial(\rho\mathbf{v})/\partial t &= -\nabla\cdot(\rho\mathbf{v}\mathbf{v}) - \nabla p + \mathbf{j}\times\mathbf{B} \\ \partial\mathbf{B}/\partial t &= \nabla\times(\mathbf{v}\times\mathbf{B} - \eta\,\mathbf{j}) \\ \partial p/\partial t &= -\nabla\cdot(p\mathbf{v}) - (\gamma-1)\,p\,\nabla\cdot\mathbf{v} + (\gamma-1)\,\eta\,\mathbf{j}^{\,2} \end{aligned}$$

with

$$\nabla\times\mathbf{B} = \mu_0\,\mathbf{j}$$

where $\rho, p, \mathbf{v}, \mathbf{B}$, and $\mathbf{j}$ are plasma mass density, pressure, velocity, magnetic field and current density, respectively.

In our simulation, plasma density, magnetic field, and length are normalized by $\rho_0 = m_i \times 10^6\ (kg\ m^{-3}), B_0 = 20 \times 10^{-9}\ (Tesla), L_0 = 1\ (Re) = 6370\ (km)$ where m_i is the mass of a proton. Other normalizations follow from these units; $v_0 = B_0^2/\sqrt{\mu_0\rho_0} = 436.6\ (km/s), t_0 = L_0/v_0 = 14.6\ (sec), p_0 = \rho_0 v_0^2 = 3.18 \times 10^{-10}\ (Jm^{-3}), j_0 = {\mu_0}^{-1}B_0/L_0 = 2.50 \times 10^{-9}\ (Am^{-2})$. We solve these MHD equations numerically using a recently developed three-dimensional high-precision code [Watanabe and Sato, 1990] in which the Runge-Kutta-Gill method for time advance and the direct difference method in space are adopted.

The simulation box is defined over

$$-100\ Re \le x \le 20\ Re,\ 0 \le y \le 50\ Re,\ 0 \le z \le 50\ Re$$

where the x axis is along the sun/earth line with the positive direction pointing towards the sun; the y axis is along the dawn/dusk line; and the z axis directs north.

An initial magnetic field is produced by the superposition of the earth's dipole moment placed at the origin and directed northward and it's image dipole moment placed at $(x = 40, y = 0, z = 0)$ so that perpendicular field lines at the sun boundary $(x = 20)$ do not exist. Such lines would remain forever because they are parallel to the solar wind flow. Use of this image dipole field was shown not to influence the results [Watanabe and Sato,1990]. This initial magnetic field is filled with a plasma of constant pressure (0.1 in normalized units). The initial density distribution was chosen so that Alfvén wave velocity is a constant ($V_{A0} = 700\ km/sec$) over the entire simulation box except for very near the earth.

The solar wind, blowing perpendicularly to the dipole moment from the sunward boundary $(x = 20)$, is introduced at the beginning of the simulation run. Soon after about 70 sec, the solar wind at the boundary reaches a stationary state in which

$$v_s = 300\ (km/sec),\ \rho_s = 5 \times 10^6 \times m_i\ (kg\ m^{-3}),\ T_s = 20\ (eV).$$

The system is symmetric about the $z = 0$ and $y = 0$ planes. Therefore mirror and anti-mirror boundary conditions are adopted at these boundaries. On the north and the side boundaries $(y = 50, z = 50)$, we used angled free boundary condition that enables deflected solar wind to get easily out of the system. By "angled free" boundary, we mean that all physical quantities have zero gradient not perpendicular to the boundary, as is usually meant by a free boundary, but rather the zero gradient is directed along some non-right angle (about 30°) which is almost parallel to bow shock at the boundary. The usual free boundary condition are assumed at the tail boundary $(x = -100)$ until the magnetosphere formation is completed. After, the pressure boundary condition is fixed to a small value (0.01 in the normalized units). The reason for this will be explained in detail in section 3.

If one wants to simulate the whole magnetosphere region consistently, magnetosphere-ionosphere coupling as well as solar wind-magnetosphere coupling should be considered at the same time. But the typical scale length of the magnetosphere

($\geq 10Re$) is so different from the ionosphere's ($\leq 100\ km$) that it is obviously impossible to handle these two interactions in the same code. Therefore we approximate the ionosphere by a resistive shell region spanning a distance between $5Re$ and $8Re$. The inner sphere of radius $5Re$ is not included in our calculation.

We divide this simulation box into $185 \times 69 \times 69$ meshpoints with the spacing between grid points increasing with distance from the earth. This was done in order to use as large a physical simulation region as possible while maintaining numerical accuracy. Fig.1 shows the grid points used in this study on the $y = 0$ and the $z = 0$ planes. Only odd number grids are drawn for easy viewing. In the near earth region, the mesh size has a minimum value of $0.50Re$ and goes to a maximum value of $1.11Re$ at the tail boundary. At the near-earth plasma sheet where magnetic reconnection occurs ($x \sim -20$) the mesh sizes in x,y,and z directions are respectively $0.54Re$, $0.50Re$ and $0.50Re$.

The time step Δt is determined by the smallest grid size $\Delta x = 0.50Re$ and the initial constant Alfvén wave speed $V_{A0} = 700\ km/s$ as $V_{A0} = 0.8\ \Delta x/\Delta t$ and its value is 0.25 in normalized units. The high-precision code used in this study permits such a large time step and is one of its merits. Thus we may observe processes of the magnetosphere on the scale of hours. Watanabe and Sato [1990] analyzed, in detail, this code.

3 Simulation Results

As soon as the solar wind is injected at the beginning of the run, it's dynamic pressure deforms the dipole filed. About 1.5 hours later we obtain a three dimensional magnetosphere with a clear bow shock, magnetopause, high temperature plasma sheet and distant tail ($\leq 100Re$). Afterward, near-earth reconnections occur in the plasma sheet giving rise to the formation of several plasmoids which are ejected tailward.

We chose a constant resistivity (magnetic Reynolds number $S \sim 1000$) in the region ($x \leq -9.8,\ y \leq 13,\ z \leq 5$) that approximately corresponds to the plasma sheet. This constant resistivity is so small that its value is comparable to numerical resistivity.

For two different reasons, we numerically damped two regions of the simulation

box. The first consists of the region $x \geq 12.4$ almost in front of the bow shock ($x \sim 13$). If it were not for this damping region, the tip of the magnetopause ($x \sim 11$) would deform out of shape due to accumulated numerical error which is particularly large at the dayside point of the magnetopause. This is because the physical quantities vary greatly over very short distances here. The second damping is necessary to facilitate a fast formation of the magnetosphere. We hope to observe the formation of a 3-D magnetosphere from an initial dipole field. But during the transformation, a return (sunward) flow occurs behind the earth in the region that is near the sun/earth axis for $x \leq -20 \sim -30$. This return flow deforms the magnetic field in the plasma sheet near the x axis so that resulting configuration is far from the expected magnetospheric configuration. Therefore we softly damp the sunward flow (flow which has a positive x component) by 5 % in the region $x \leq -20$ and gradually remove this damping region so that it never overlaps the plasmoid. By $t = 4.06$ hours, we completely remove this damping region.

Fig.2 shows the time development of magnetospheric formation and subsequent near-earth reconnections and plasmoid ejections for the meridian cross section where positive x is left and positive z upward. These figures depict the region ($20 \geq x \geq -100$, $40 \geq z \geq -40$) although the simulation region in the z direction is ($50 \geq z \geq 0$). The negative z region is drawn using mirror conditions. Fig.2(A) to (P) show time development from t=0.51 hours to t=8.11 hours with an even time interval of 0.51 hours. The solid, thick lines depict the magnetic field lines which are tied to the earth. The dashed lines depict the field lines which penetrate the equatorial plane southward i.e., the reconnected field lines that drape the plasmoid. Each field line is drawn only when the magnetic field is larger than 1 nT. The solar wind flow is depicted by thin, solid lines.

The bow shock can be clearly seen from these figures by the flow lines that are abruptly deflected. On the sun/earth axis (x axis) the bow shock is located at about $x \sim 13$. The magnetopause, which forms tangential discontinuity, is also clearly seen. The dayside magnetopause is located about $x \sim 11$.

At t = 0.51 hours (Fig.2(A)), we can see that only the front part of the magnetosphere has formed. At $t = 1.52$ hours (Fig.2(C)), the magnetosphere formation has almost finished all the way to the end of the far magnetotail ($x \geq$

-100).

By this time, the plasma sheet has been formed. The formation process of the plasma sheet has been well studied in the previous global simulation [Watanabe and Sato, 1990]. The solar wind, in compressing the earth's magnetic field, drives large amplitude magnetosonic waves. These waves propagate in the north lobe and south lobe and collide at the equatorial plane. The plasma in this region is heated by adiabatic compression due to these waves. This region eventually develops into the plasma sheet. The plasma sheet is broad in the equatorial plane though quite thin in the meridian plane.

Fig.3 shows the pressure and the temperature profiles along the x axis and the corresponding contour lines on the meridian cross section at $t = 1.52$ hours. We can see from Fig.3 that the pressure and the temperature suddenly jump at $x \sim 13$ where is the bow shock front. Another peak can be seen behind the earth at $x \sim -11$ in the plasma sheet. Pressures's maximum value in the plasma sheet is 0.4 in normalized units. (Recall that the initial homogeneous pressure was 0.1.)

Note that the neutral sheet is also formed by this time. This is evident from the shape of field lines in the plasma sheet of about $15 \sim 30Re$ behind the earth in Fig.2(C). Near the equatorial plane in this region, the magnetic field is almost zero, the neutral sheet. Fig.2 (A),(B), and (C) show that the plasma sheet thins and the shape of the field lines approaches that of a neutral sheet configuration. This plasma sheet thinning is also exhibited in the pressure contour lines of Fig.3.

We consider why the neutral sheet has formed here. The behavior of this particular region is determined essentially by the large amplitude magnetosonic waves which are driven by solar wind dynamic pressure when the initial dipole field is deformed to the magnetospheric configuration. The waves in the north lobe and the south lobe collide most violently in this region. And collided plasma flows out from this region with the magnetic field lines. This is the most highly compressed region and, as a result, the magnetic field becomes very weak.

In the simulation of Watanabe and Sato, the neutral sheet did not appear and the magnetosphere became almost stationary about $t = 1.6$ hours after the formation. In our simulation, the magnetosphere is not a stationary state. However, growth rate of the instability is rather small as will be seen. Evidently, using an appropriately large simulation region enables the formation of the neutral sheet

and is key in obtaining the details of magnetosphere dynamics.

Note that this neutral sheet is in the plasma sheet where the plasma pressure is very high. Therefore, the local beta is very large ($\beta \gg 1$) in this region. In addition, compared to the pressure gradient in Fig.3(a), we see from Fig.2(C) that the field lines have 'bad curvature' in the region $x \leq -11$. So, this region can be unstable to a ballooning instability.

Finally, at $t \sim 1.6$ hours (just after Fig.2(C)) magnetic field lines begin to reconnect at the equatorial plane. Judging from the z component of the magnetic field, the neutral point is located at $x = -16$.

Immediately after this reconnection, as seems to naturally follow from Fig.2(C), small closed loops of field lines are formed (depicted by dashed lines in Fig.2(D)). Subsequently, as reconnection goes on, the flux of the closed loops increases and the tension of the loop field lines tend to make the structure roundish (Fig.2(E),(F)). Thus a plasmoid is born. It is ejected tailward by the lobe field tension force and probably by the pressure gradient force (Fig.2(G),(H)).

The plasmoid's size eventually exceeds $80Re$ along the sun/earth axis. Based on the movement of the O point, the speed of the plasmoid is about 80 to 100 km/s.

At $t \sim 4.06$ (Fig.2(H), 2.4 hours after the appearance of the neutral line) the plasmoid touches the tail boundary ($x = -100$). The positive x flow damping region explained at the head of this section is completely removed at this time. Here we mention the tail boundary condition. Initially, the boundary condition of the pressure at the tail was free. With such a boundary condition, the plasmoid rebounds slightly at the boundary and is trapped by it. This is not a realistic situation. So, we changed the pressure boundary condition of the tail to a small, fixed value (0.01) after $t = 3.04$ hours to push the plasmoid out with a pressure gradient force.

This first plasmoid almost leaves the system by $t \sim 6.08$ hours (Fig.2(L)). It is interesting to note that the magnetosphere thins compared to it's previous size. The width of the magnetosphere in the z direction (the distance from the south magnetopause to the north magnetopause) at $x = -20$ is $50Re$ at $t = 1.52$ hours (Fig.2(C)) but shrinks to $45Re$ at $t = 6.08$ hours (Fig.2(L)). The reduction at $x = -100$ is almost the same value. The cause is easy to understand. The

plasmoid takes, with it, some flux from the lobe. To balance the solar wind dynamic pressure which is almost unaffected by the magnetosphere, the lobe field magnitude on the magnetopause must be constant. This is the condition of a tangential discontinuity. So, the loss of the flux should be compensated by a decrease of area of the lobe cross section. In this way, the magnetosphere changes its energy state. We can say that the magnetosphere releases energy by ejecting a plasmoid and relaxes to a lower energy state.

To see the movement of the neutral lines in detail, Fig.4 shows the profile of log of the magnetic field strength on the x axis at $t = 2.03, 2.53, 3.04, 3.55$ and 4.06 hours. The corresponding pressure profiles are also depicted. The movement of X–points and O–points can be seen from the graph of the magnetic field. The O–point moves tailward together with the plasmoid. The X–point, on the other hand, remains in the region $(-16 \geq x \geq -27)$ and almost always near $x = -20$.

Note the peak of the pressure in the plasma sheet at $x \sim -11Re$ in Fig.4. Though the plasmoid takes out some of energy of the plasma sheet plasma, the maximum of the peak pressure of the plasma sheet increases after the plasmoid leaves. Comparing these graphs with Fig.2, we may surmise the cause of this heating. The heating seems begin at $t = 3.04$ when the grown plasmoid begins to leave the near earth region (Fig.2 (F)). As mentioned above, the plasmoid takes some magnetic flux from the lobe thus reducing the cross section of the lobe. At this moment a magnetosonic wave is driven. This magnetosonic wave propagates in the north lobe and the south lobe to the equatorial plane where these waves collide. Thus the plasma in the plasma sheet is heated by adiabatic compression. This is the same mechanism as seen in the formation of the plasma sheet.

After the first plasmoid disappears, Fig.2(L) ($t = 6.08$ hours) shows that there exists a left over of the first plasmoid. One can say that this configuration is more realistic than the configuration before the plasmoid ejection (Fig.2(C)) because, in Fig.2(C), there still exists northward magnetic field lines that penetrate the equatorial plane at the tail part. The magnetic field in Fig.2(C) is topologically same as the initial dipole field. In Fig.2(L), on the other hand, the magnetic field is closer to the expected magnetospheric configuration that has a neutral sheet. The dipole field topologically differs from the magnetic field that has a neutral sheet. So, it follows that magnetic reconnection was needed to construct

a realistic magnetosphere.

One of the most interesting findings in this study is that the plasmoid ejection does not occur only once. Fig.2(N) shows that magnetic reconnection in the plasma sheet occurs again at $x \sim -20$ and at $x \sim -50$. The reconnection proceeds at $x \sim -20$ (Fig.2(O)) and a new large plasmoid is formed and ejected (Fig.2(P))). It took about 3 hours for such a large plasmoid as depicted in Fig.2(I) to grow from its initial reconnection. The starting time of the formation of the second plasmoid is rather ambiguous but if we suppose that it begins at Fig.2(M), only about half as long is needed for the second plasmoid to grow to the same size (Fig.2(P)). This is probably explained by the topological difference of the magnetic configuration explained above.

It is interesting to note that the Kelvin-Helmholtz type instability does not occur on the magnetopause through the run and the solar wind does not enter into the magnetosphere through the magnetopause.

The latitude of earth's surface point that is connected by a field line to the near-earth reconnection point on the meridian plane is located between 64.1° to 64.5° in latitude throughout the run.

Now we examine the time sequence of the formation and the ejection of the plasmoid on the equatorial cross section. Fig.5 shows the velocity vectors together with magnetic neutral lines on the equatorial plane. The magnetic field has southward component in the region surrounded by these neutral lines. Fig.5(A) to (P) correspond to Fig.2(A) to (P). At $t = 0.51$ hours (Fig.5(A)), the magnetosphere is under construction. We can clearly see the bow shock from the sudden redirection of the velocity vectors of the solar wind. The solar wind seems to enter deeply into the tail part of the pre-magnetosphere, but the 'frozen in' condition inhibits such a invasion of the plasma flow into the magnetic field. These vectors should be interpreted as the flow of the inner magnetospheric plasma moving with the magnetic field lines that are violently deforming. At this time we can also see the plasma flow going around the earth from the plasma sheet towards the dayside. This flow is transient and exists only when the front part of the magnetosphere is under formation.

We showed the magnetic field lines on the meridian cross section in Fig.2, and saw that near-earth reconnection did not yet occur at $t = 1.52$ hours (Fig.2(C)).

However, Fig.5(B) shows that magnetic reconnection occurs, on the sidelines, already at $t = 1.01$ hours. This reconnection cannot be seen from the meridian plane. Near-earth reconnection usually refers to reconnection occurring on the meridian plane. This 'sideline' reconnection is probably not important to processes in the real magnetosphere. We assumed an initial dipole field in order to construct a magnetosphere. The real magnetosphere, of course, does not experience such a formation process. Compared to Fig.5(A), we can see that the 'sideline' reconnections in Fig.5(B) are located where the transient flows appeared. These flows may transport magnetic field lines and weaken the field strength there and thus reconnection can easily occur. So, this sideline reconnection relates directly to the magnetosphere formation process which plays a central role in our simulation but would not occur in the real magnetosphere. There are other neutral lines of the same type at the tail at $t = 1.52$ hours (Fig.5(C)).

Fig.5(D) ($t = 2.03$ hours) shows that there are two neutral lines crossing the x (sun/earth) axis. These lines represent the X-line and the O-line of the (real, center field) plasmoid that appears in the meridian cross section (Fig.2(D)). Fig.5(E)–(G) shows the growing process of this plasmoid. It spreads over in the y (dawn/dusk) direction as well as in the x direction. The plasmoid movement is shown in the tailward velocity vectors. Comparing vectors, it can be seen that the plasmoid velocity is not faster than the solar wind velocity (300 km/s). The sunward flows are produced by reconnection at $x \sim -20$. They are deflected by the hard core of the dipole-like magnetic field at $x \sim -13$ and go around it (for example, Fig.5(G)). Note that this sunward flow is not damped by the positive x flow damping explained at the head of this section. In Fig.5(K) to (M), it seems that the neutral lines spread over the plasma sheet. The magnetic field in the region surrounded by these neutral lines have a negative z component (southward direction). However its magnitude is very weak; almost zero. (Recall that the magnetic field lines in Fig.2 are drawn only when its magnitude is larger than $1nT$.) Fig.5 shows that the width in the y direction of the magnetosphere is highly reduced after the first plasmoid is ejected. Judging from the flow line positions (not depicted), the width decreases to $10Re$ in radius. The 'sideline' reconnection occurring in the plasma sheet could be a cause of this phenomenon since this reconnection brings flux in the side of the magnetosphere.

There is no clear distribution of field aligned current on the y-z cross section near the reconnection point. The absence of the IMF may explain this fact. If a southward IMF is injected and dayside reconnection occurs, reconnected IMF lines eventually drape the magnetosphere. These field lines will apply a force on the plasma sheet through the lobes. If near-earth reconnections occur under this condition, it may be regarded as a driven reconnection. In such a case, field aligned currents may be produced as predicted by local simulations [Sato et al., 1981].

Fig.6(A) and (B) show the three dimensional structure of plasmoids at $t = 3.04, 4.06, 7.10$ and 8.11 hours. The solid lines depict the field lines that have negative z component on the equatorial plane. The 'sideline' reconnections can be seen at $t = 3.04$ hours. However, reconnection occurring near the meridian plane produce a large plasmoid and it become dominant (at $t = 4.06$ hours). Then reconnections occurs again in the plasma sheet ($t = 7.10$) and the second plasmoid is formed ($t = 8.11$).

4 Summary

We have performed a global 3-D MHD simulation of the magnetosphere involving the distant tail (to $100Re$). We observed the formation of three dimensional magnetosphere from an initial dipole field under the dynamic pressure of the solar wind (no IMF) within 1.5 hours. This magnetosphere has a neutral sheet unlike a previous global simulation in which the tail extended only to $60Re$. A global simulation extending only to $60Re$ in the tailward direction is not sufficiently large to simulate a realistic magnetosphere.

The magnetosphere formed in this simulation is not in a stationary state. The plasma sheet in the region $x = -15$ to $-30Re$ continues to thin and finally, at $t = 1.62$ hours, magnetic field reconnection occurs in the plasma sheet at about $x = -20Re$ on the meridian plane. Though a small constant resistivity is assumed in the plasma sheet (magnetic Reynolds number ~ 1000), no artificial methods are imposed to trigger the reconnection.

This particular region $x = -15$ to $-30Re$ is determined by the large amplitude magnetosonic waves which are driven by the solar wind dynamic pressure when

the initial dipole field is deformed into the shape of the magnetosphere. The waves propagate in the north lobe and the south lobe and collide most violently in this region. As a result, the plasma in this region is heated up by adiabatic compression (plasma sheet formation) and the magnetic field become very week (neutral sheet formation). Accordingly the local beta in this region become very large and it makes the plasma unstable. Thus reconnection occurs in this region.

As a result of this near-earth reconnection, a plasmoid is produced and ejected tailward. It's size grows to more than $80Re$ and its speed is about $80 - 100\ km/sec$. This plasmoid leaves the simulation box at $t = 6.08$ hours. After this plasmoid ejection, the width of the magnetosphere reduces by about 5 Re. The ejecting plasmoid takes flux from the lobe field out the system with it, thus causing this reduction in magnetosphere width.

The neutral point in the plasma sheet is located at about $x \sim -20Re$ throughout the ejection processes of the plasmoid. The point on the surface of the earth that is connected to the neutral point by a magnetic field line is at about 64.1° to 64.5° in latitude.

The pressure peak in the plasma sheet ($x \sim -11Re$) is observed to increased after the ejection of a plasmoid. Adiabatic compression of the plasma sheet after the plasmoid ejection explains this heating effect.

A field-aligned current produced by the reconnection is not clearly observed. The absence of an IMF may explain this effects. Because the driving force of this reconnection is far less than if IMF were included.

The ejection of the first plasmoid was followed by a second reconnection and plasmoid ejection. The growth time of the second plasmoid is about half of the first one. This fact may be explained by the topological difference of the magnetic field.

In addition, the three dimensional structure of plasmoids are shown.

This simulation shows that the magnetosphere configuration having a neutral sheet and sufficiently long tail is slightly unstable when the tail is formed after interacting with a solar wind flow without an IMF. The time scale of plasmoid's formation and ejection is more than several hours and it seems too long compared to observed, isolated substorms. One can expect that a disturbance may trigger the near-earth reconnection much more rapidly. An interplanetary shock or a

southward turning of the IMF is a candidate for such triggers. In fact, magnetospheric substorms are often observed tens of minutes after a southward turning of the IMF. If we perform a global simulation which includes the southward IMF, through dayside reconnection, the IMF would drape the magnetosphere and apply a force on the plasma sheet through the lobes. Then both the near-earth reconnection rate and driving force of plasmoid ejection will be increased. So, the next step in understanding the dynamics of the magnetosphere is to consider the effects of the IMF. This work will be published in the near future.

Acknowledgements

The authors wish to thank Professor K.Nishikawa for encouragement throughout this work. The authors are also grateful to Mr. A.Usadi for valuable discussions.

References

Hayashi,T., and T.Sato, Magnetic reconnection: Acceleration,heating, and shock formation, *J. Geophys. Res., 83*, 217,1978.

Hones, E.W.,Jr., Substorm processes in the magnetotail: comments on 'On hot tenuous plasmas, fireballs, and boundary layers in the Earth's magnetotail' by L.A.Frank, K.L.Ackerson, and R.P.Lepping, *J. Geophys. Res. 82*, 5633, 1977.

Sato,T., R.J.Walker, and M.Ashour-Abdalla, Driven magnetic reconnection in three dimensions: Energy conversion and field-aligned current generation, *J. Geophys. Res. 89*, 9861, 1984.

Slavin,J.A., D.N.Baker, J.D.Craven, R.C.Elphic, D.H.Fairfield, L.A.Frank, A.B.Galvin, W.J.Hughes, R.H.Manka, D.G.Mitchell, I.G.Richardson, T.R.Sanderson, D.J.Sibeck, E.J.Smith, and R.D.Zwickl, CDAW 8 observations of plasmoid signatures in the geomagnetic tail: An assessment, *J. Geophys. Res. 94*, 15153, 1989.

Watanabe,K., and T.Sato, Global simulation of the solar wind-magnetosphere interaction: the importance of its numerical validity, *J. Geophys. Res., 95*, 75, 1990.

Figure Captions

Fig.1 Numerical mesh used in the simulation. Grid points are drawn here on the meridian and the equatorial planes. The simulation box is divided into $185 \times 69 \times 69$ mesh points with the spacing between grid points increasing with distance from the earth.

Fig.2 Time development of the magnetosphere for the meridian cross section where positive x is left and positive z upward. The solid, thick lines depict the magnetic field which are tied to the earth. The dashed lines depict the reconnected field lines that drape the plasmoid. The solar wind flow is depicted by thin, solid lines.

Fig.3 The pressure and the temperature profile on the sun/earth axis and their contour lines on the meridian plane at $t = 1.52$ hours.

Fig.4 Profiles of the magnetic field and the pressure on the sun/earth axis at $t = 2.03, 2.53, 3.04, 3.55$ and 4.06 hours.

Fig.5 The velocity vectors together with magnetic neutral lines on the equatorial plane where (A) to (P) correspond to Fig.2(A) to (P).

Fig.6 Three dimensional structure of plasmoids. The solid lines depict the magnetic field lines that penetrate the equatorial plane southward. The earth is depicted by a circle.

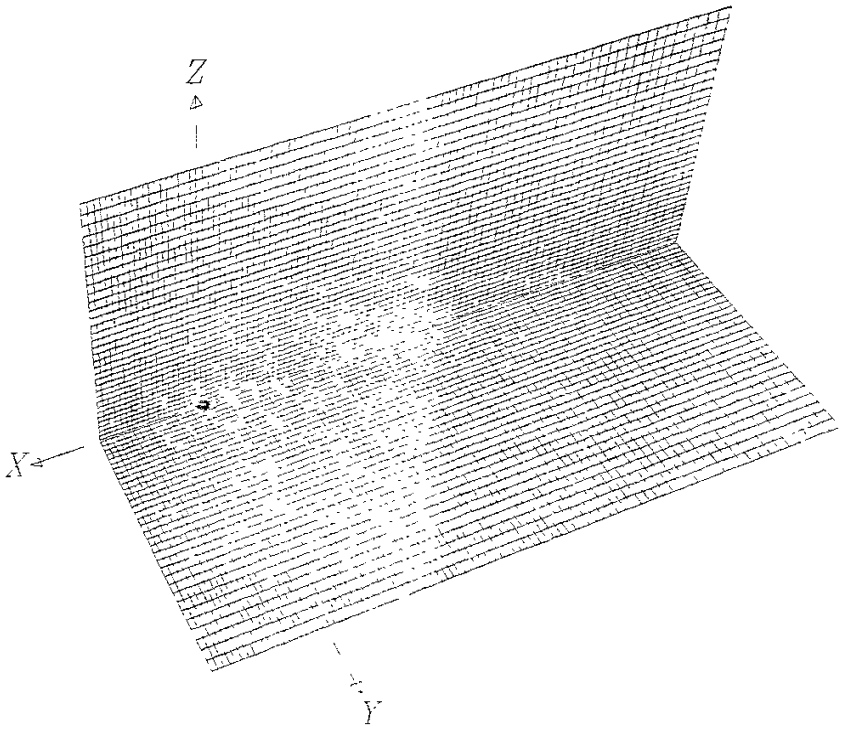

Fig.1

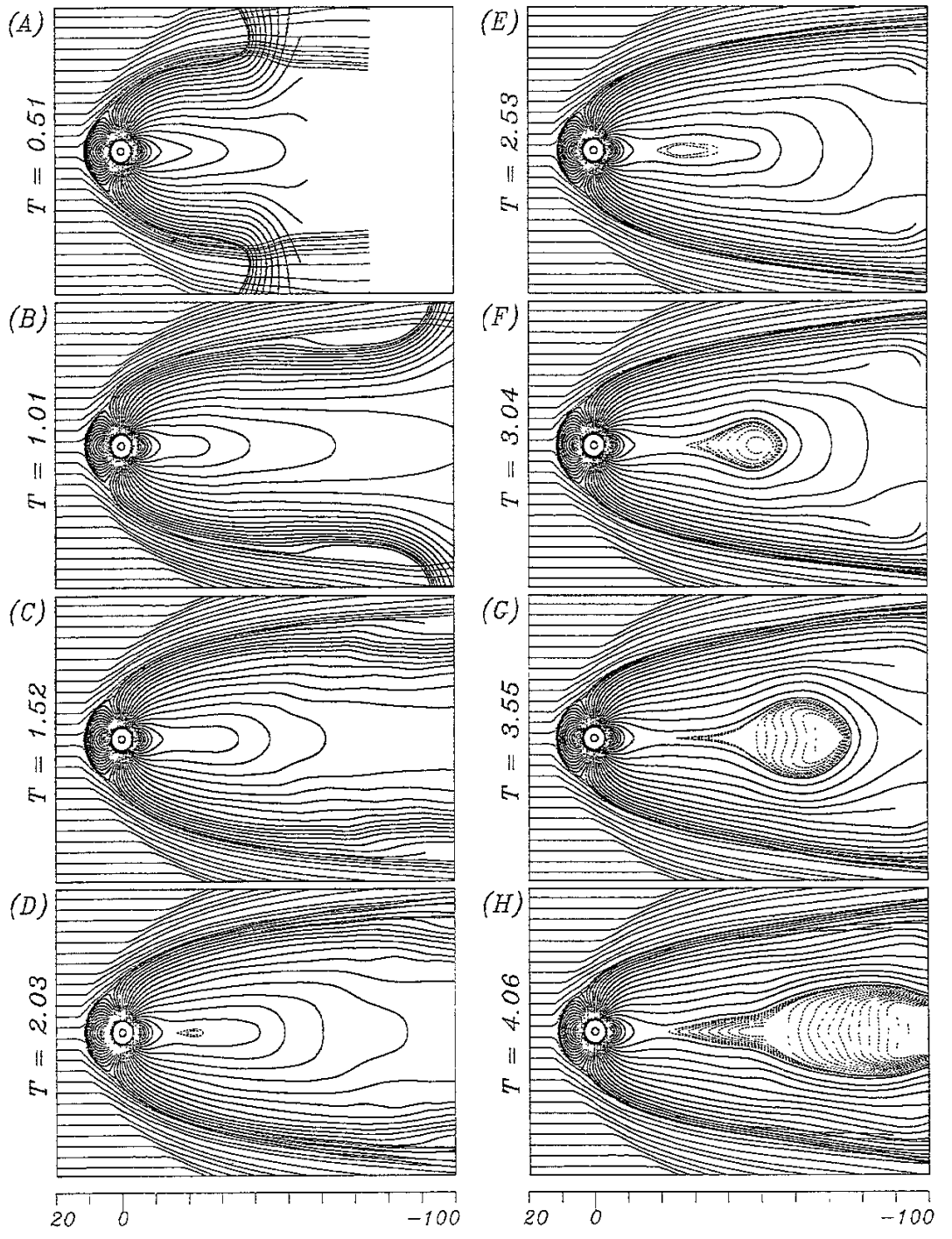
(A)
T = 0.51
(B)
T = 1.01
(C)
T = 1.52
(D)
T = 2.03
(E)
T = 2.53
(F)
T = 3.04
(G)
T = 3.55
(H)
T = 4.06
20
0
−100
20
0
−100

Fig.2(A)–(H)

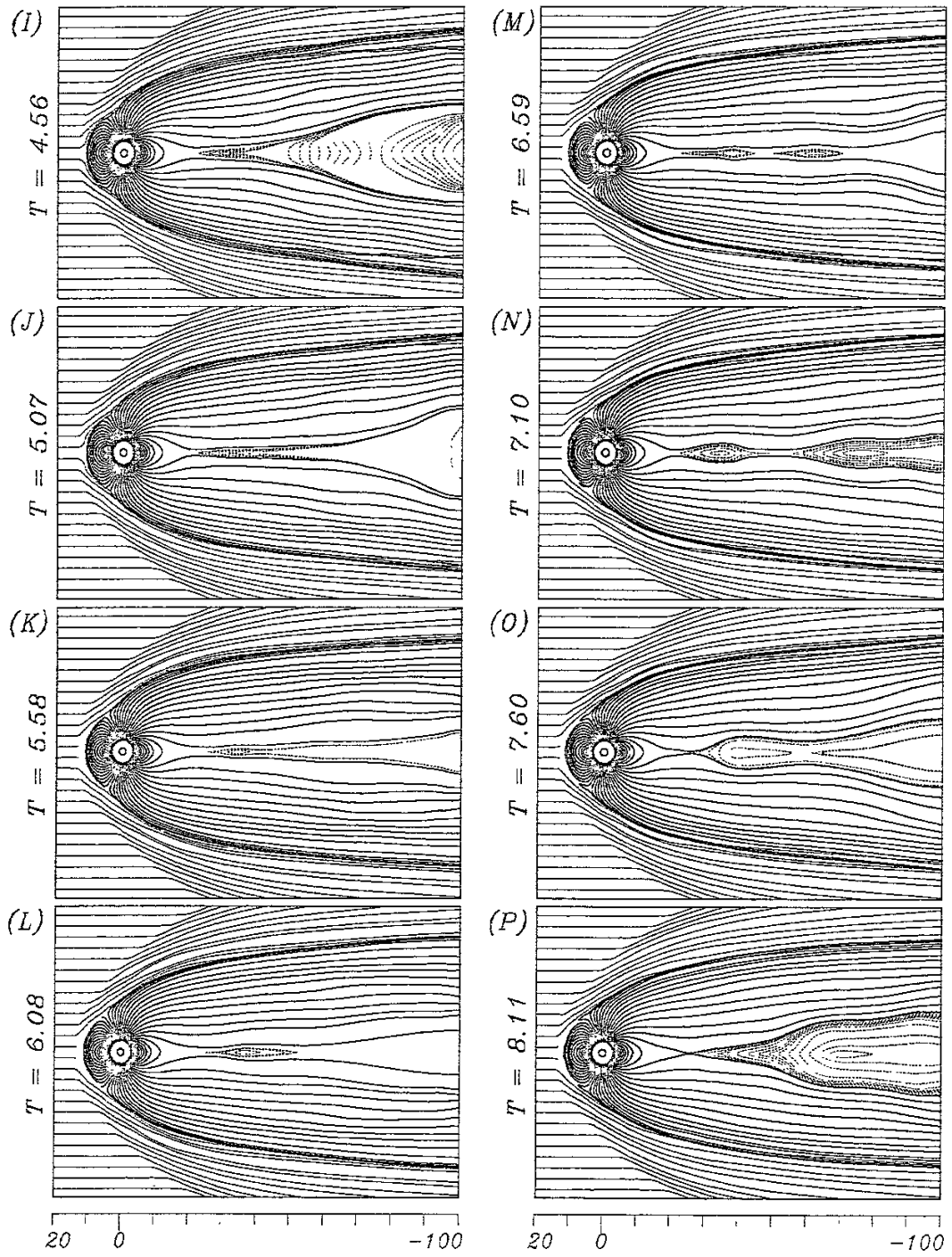
(I)
T = 4.56
(J)
T = 5.07
(K)
T = 5.58
(L)
T = 6.08
(M)
T = 6.59
(N)
T = 7.10
(O)
T = 7.60
(P)
T = 8.11
20
0
−100
20
0
−100

Fig.2(I)–(P)

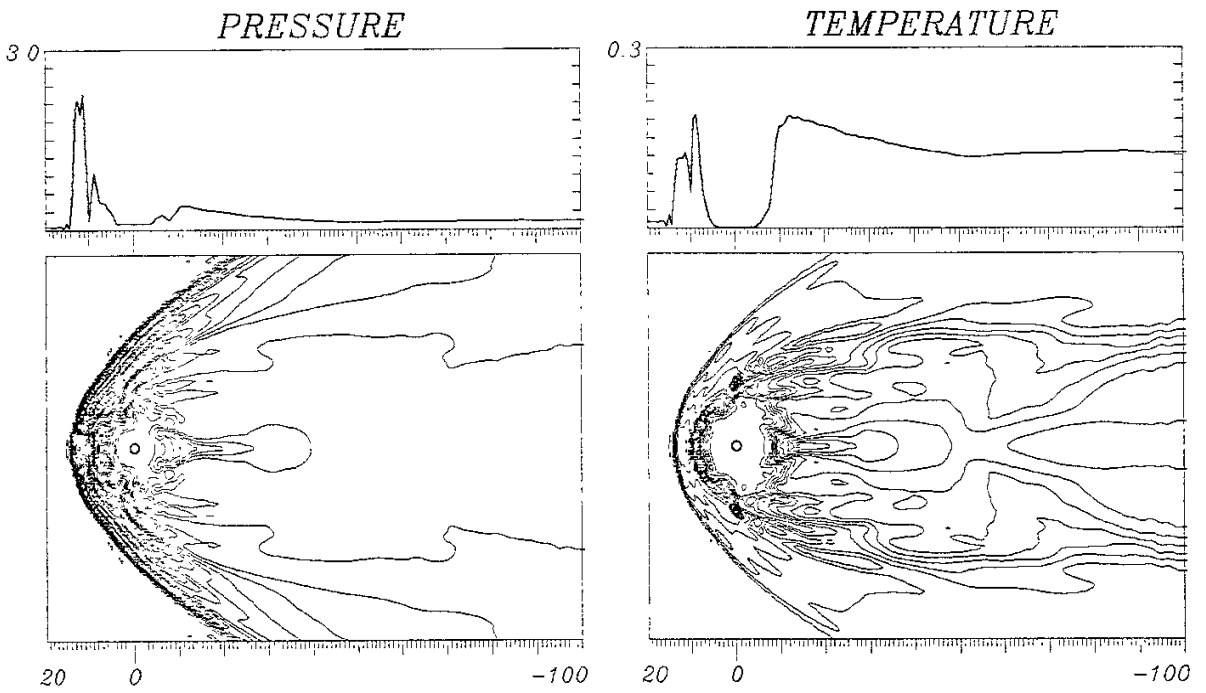

Fig.3

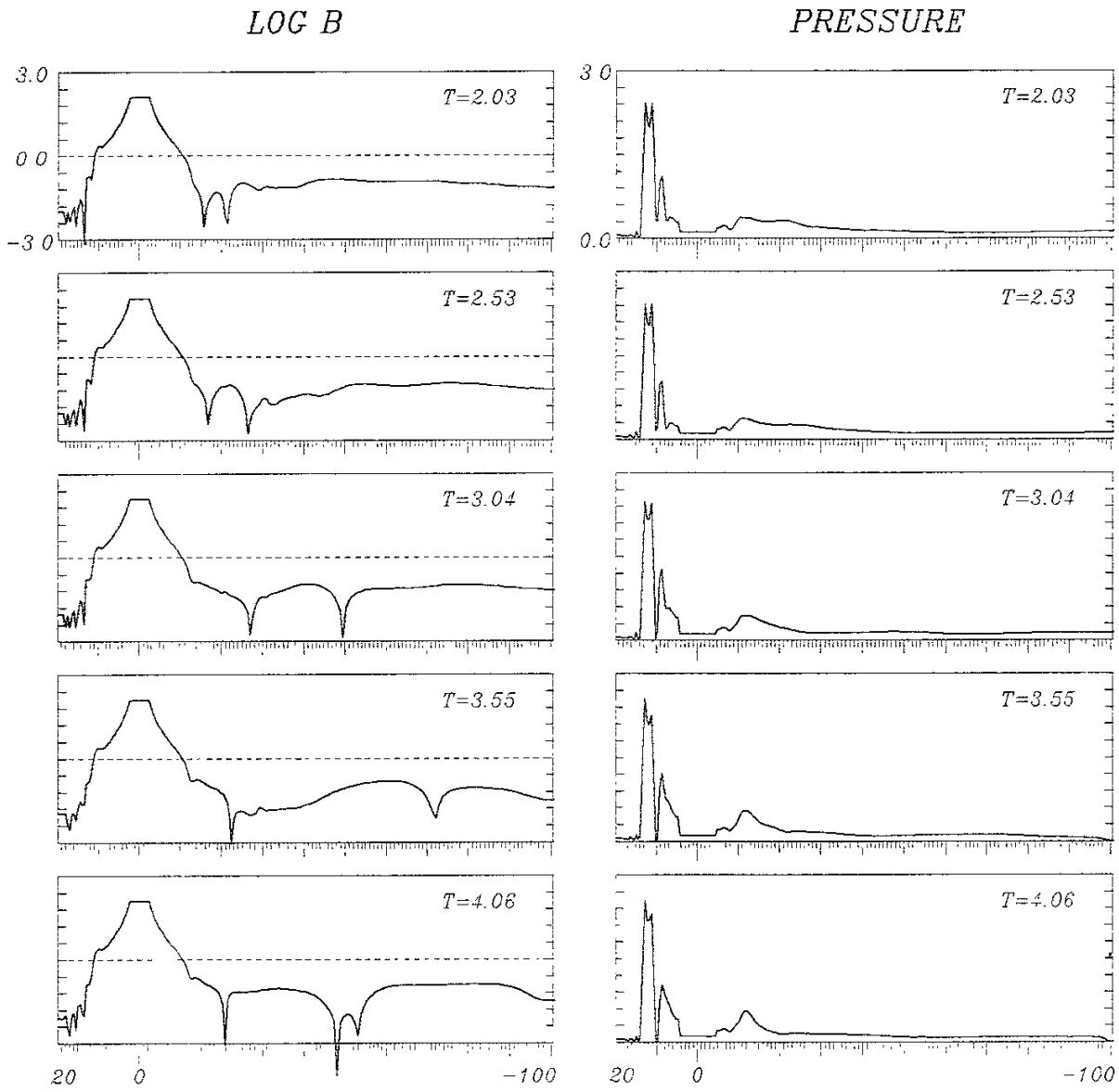

Fig.4

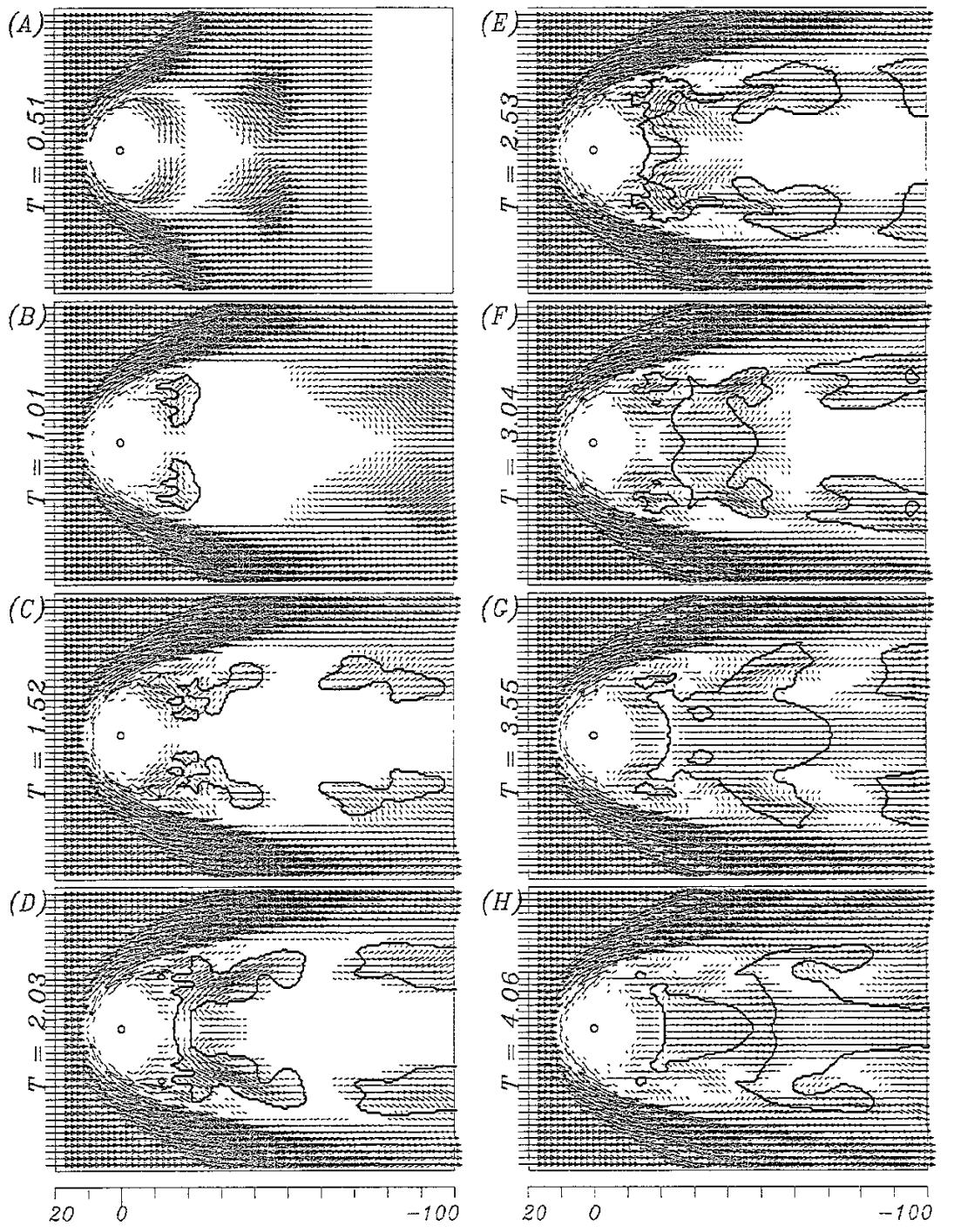
(A)
T = 0.51
(B)
T = 1.01
(C)
T = 1.52
(D)
T = 2.03
(E)
T = 2.53
(F)
T = 3.04
(G)
T = 3.55
(H)
T = 4.06
20
0
−100
20
0
−100

Fig.5(A)-(H)

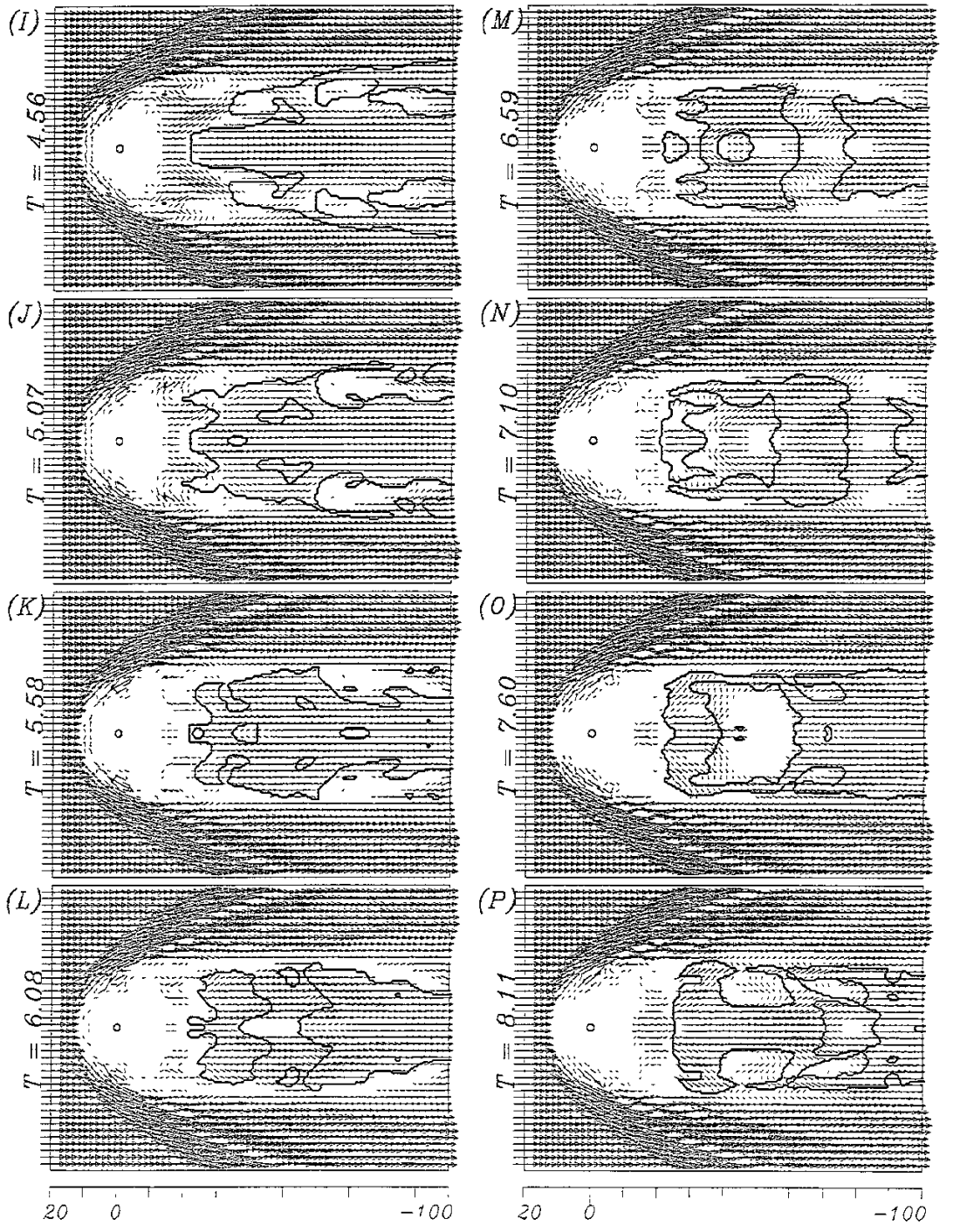
(I)
T = 4.56
(J)
T = 5.07
(K)
T = 5.58
(L)
T = 6.08
(M)
T = 6.59
(N)
T = 7.10
(O)
T = 7.60
(P)
T = 8.11
20
0
−100
20
0
−100

Fig.5(I)-(P)

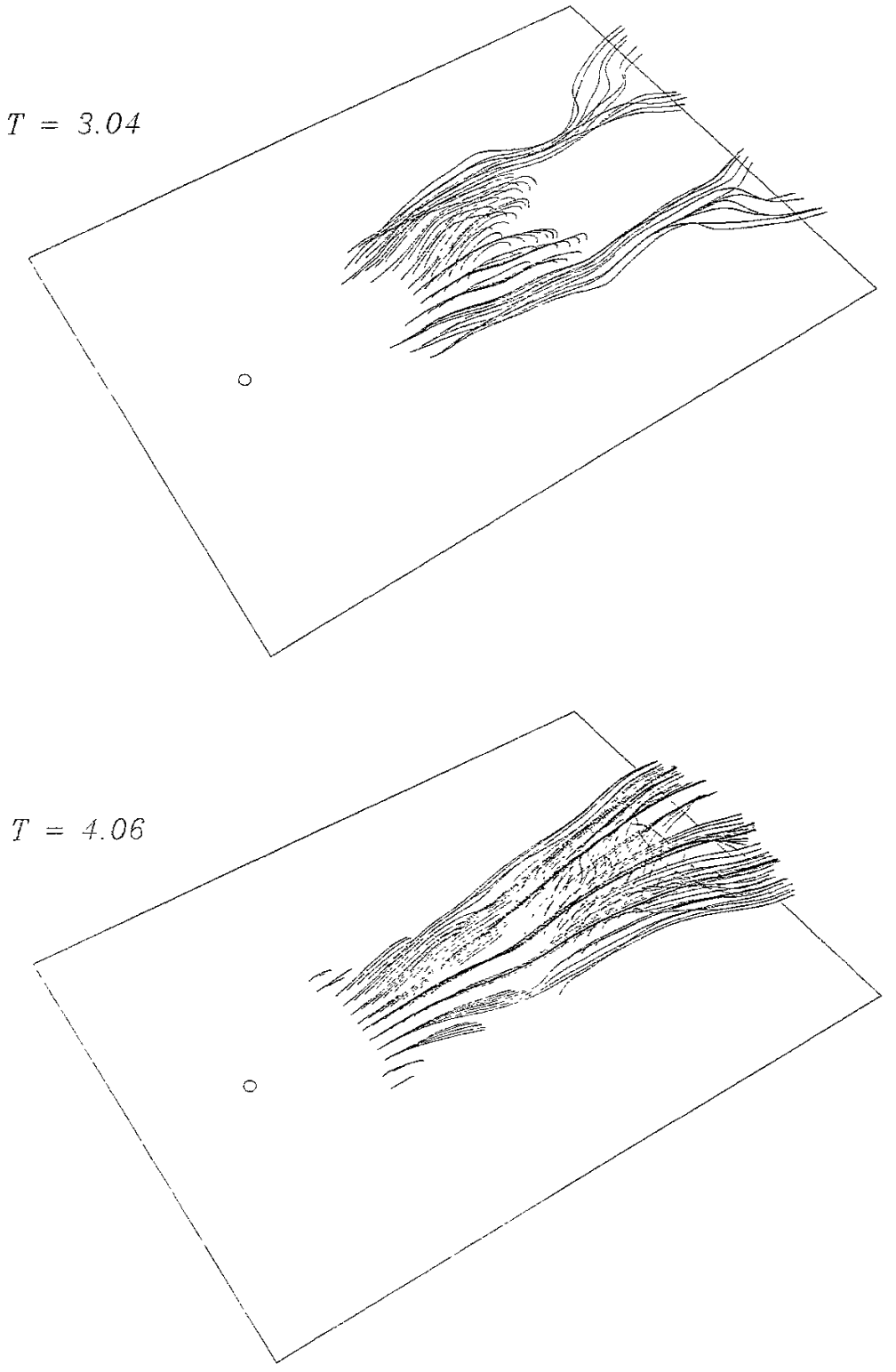

Fig.6(A)

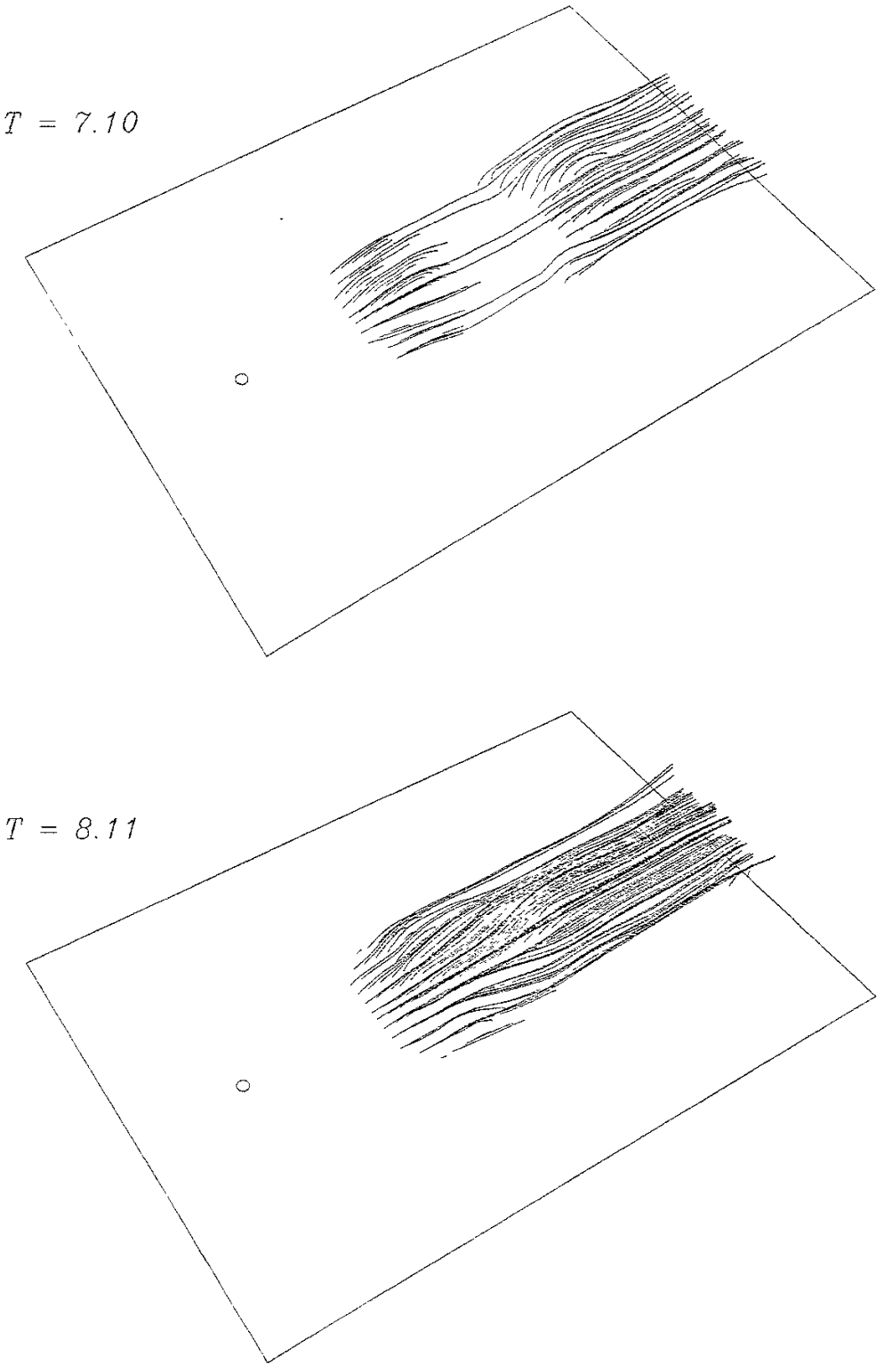

Fig.6(B)